PROCEEDINGS OF SPIE

SPIEDigitalLibrary.org/conference-proceedings-of-spie

Inverse opal TiO2-based heterocomposite photonic structures for slow photon-assisted visible light photocatalysis

Madanu, Thomas, Mouchet, Sébastien, Deparis, Olivier, Su, Bao-Lian

Thomas L. Madanu, Sébastien R. Mouchet, Olivier Deparis, Bao-Lian Su, "Inverse opal TiO2-based heterocomposite photonic structures for slow photon-assisted visible light photocatalysis," Proc. SPIE 12150, Photonics for Solar Energy Systems IX, 1215004 (24 May 2022); doi: 10.1117/12.2625327

SPIE.

Event: SPIE Photonics Europe, 2022, Strasbourg, France

Inverse opal TiO_2-based heterocomposite photonic structures for slow photon-assisted visible light photocatalysis

Thomas L. Madanu*[a,c], Sébastien R. Mouchet[b,c,d], Olivier Deparis[b,c], Bao-Lian Su*[a,c,e]
[a]Laboratory of Inorganic Materials Chemistry (CMI), University of Namur; [b]Solid-State Physics Laboratory (LPS), University of Namur; [c]Namur Institute of Structured Matter (NISM), University of Namur, Rue de Bruxelles, 61, 5000 Namur, Belgium; [d]Department of Physics and Astronomy, University of Exeter, Stocker Road, Exeter EX4 4QL, United Kingdom; [e]State Key Laboratory of Advanced Technology for Material Synthesis and Processing, Wuhan University of Technology, Wuhan, 430070, Hubei, China

ABSTRACT

Manipulation of light was proved to be an efficient strategy to improve light harvesting efficiency in solar energy conversion. Inverse opal (IO) photonic structures are among the most promising materials, which permit light manipulation, thanks to their ability to slow down light at specific wavelengths and localize it within the dielectric structure. However, the generation, the control and, in particular, the practical utilization of these narrow spectral range 'slow photons' remain highly challenging and relatively underexplored. In this work, we report the ability not only to generate slow photons in the visible range by synthesizing highly ordered IO TiO_2 photonic structures, but also to control and tune their wavelengths, by varying lattice parameters (pore sizes), such that they can be efficiently utilized by the composite bismuth (Bi)-based semiconductor for visible light photocatalysis. Photocatalytic experiments revealed a 70% increase in efficiency in all IO structures compared to the corresponding non-structured compact film. In addition, a 20% increase in efficiency was observed when the photonic stop band gap as well as its blue and red edges were accurately tuned to match the electronic absorption of the Bi-based photocatalyst. Our choice of IO synthesis parameters and tuning strategies enabled us to generate, control and transfer the energy of slow photons from IO TiO_2 to the composite visible light-responsive photocatalyst for highly amplified photoactivity. This work opens new possibilities for the practical utilization of slow photon effect under visible light in various solar energy conversion applications.

Keywords: Photonic crystal, inverse opal, stop band gap, slow photons, solar energy conversion, TiO_2, photocatalysis, visible light

1. INTRODUCTION

'Sustainable and CO_2-emission-free energy' has garnered extensive research interest and financial investment in the past few decades as the global drive towards reducing fossil-fuel dependency and minimizing carbon dioxide emissions continues to expand. Photocatalysis, a process involving photon-to-chemical energy conversion, is one of the most promising routes towards achieving this objective since sustainable solar energy can be harvested for 'clean' energy-related applications like water splitting for H_2 production and CO_2 reduction. Various approaches have been followed by researchers in photocatalysis in order to improve different aspects of photocatalysis like light harvesting, electron-hole pair separation, electron transport and mass transport. These approaches include synthesis of novel photocatalyst systems, modification of chemical composition of photocatalyst, modification of morphology, reaction-specific 'band gap engineering' and development of efficient photoreactors[1,2].

Although significant progress has been made using the above methods, alternative and synergistic approaches involving the manipulation of light to improve photocatalytic efficiency have not been sufficiently explored. Photonic crystals are among the promising materials that permit the control of the flow of light, thanks to their periodic structures with alternating refractive indices[3,4].

*thomas-lourdu-madanu@unamur.be; phone +32499248678; bao-lian.su@unamur.be; phone +3281724531

Photonics for Solar Energy Systems IX, edited by Alexander N. Sprafke, Jan Christoph Goldschmidt, Luana Mazzarella, Proc. of SPIE Vol. 12150, 1215004 · © 2022 SPIE · 0277-786X · doi: 10.1117/12.2625327

Under suitable conditions of high refractive index (RI) contrast and the size of periodicity corresponding to the wavelength of light, these structures reflect light within a specific wavelength range, giving rise to a photonic stop band gap (SBG), while simultaneously reducing the group velocity of light at both the blue and red edges of the SBG to nearly zero i.e., standing waves of light. The blue edge slow photons are preferentially localized in the lower RI medium, while the red edge slow photons are preferentially localized in the higher RI medium[5]. These slow photons, due to their increased optical path length and life time within the photocatalyst, can be utilized to improve energy conversion, specifically light harvesting and photocatalytic efficiency, provided the wavelengths of slow photons are accurately tuned to the electronic band gap of the photocatalyst. The tuning of slow photon wavelengths can be achieved by modifying various parameters like Bravais lattice type, lattice constant, refractive index, filling fraction, crystallographic orientation and light incident angle[6].

Various efforts have been made to exploit slow photons in photocatalysis starting from the initial work to demonstrate slow photon effect using IO TiO_2 (IOT) for the solid-phase photodegradation of methylene blue by varying both lattice parameters (pore sizes of the IOs) and incidence angle[7]. Ever since, efforts have been made to utilize inverse opal (IO) structures of various semiconductors like ZnO, WO_3, Fe_2O_3, gC_3N_4 for photocatalytic applications[8]. However, in most cases, the slow photon effect was claimed but not sufficiently established[9]. Moreover, most of the above cited works were limited either to UV-responsive photocatalysts, single-component photocatalysts or non-aqueous phase photocatalysis. In this work, we report, in a composite IOT -Bi-based (IOTB) semiconductor photocatalyst, not only the possibility to generate slow photons by synthesizing highly ordered structures but also to tune their wavelengths to the electronic absorption edge of the visible-light-responsive photocatalyst in aqueous phase. The results of our experiments indicated a 70% increase in photodegradation efficiency of all IO photocatalyst with respect to the non-structured compact film. In addition, a further 20% increase in activity under accurate tuning conditions confirmed that slow light can be efficiently utilized for photocatalysis using IO photonic semiconductors and that this approach can be extended to other applications of photonics for energy conversion.

2. EXPERIMENTAL METHODS AND SYNTHESIS

This section describes the synthesis process of the photocatalysts used in this work as well as the characterization methods and the photocatalytic test we performed.

2.1 Synthesis of IOT photonic structures

IOT films were synthesized by a colloidal templating strategy that includes a two-step process of simultaneously assembling the colloids and the phase-controlled TiO_2 nanoparticles on a glass substrate by Evaporation-Assisted Co-Assembly (EACA) method and the subsequent removal of the template by calcination[10]. In a typical process, 0.1 % dispersion of monodisperse polystyrene (PS) colloids in water and a previously prepared dispersion of phase-controlled TiO_2 nanoparticles in water were mixed together at a 25:1 ratio. A glass substrate previously treated with piranha solution (H_2SO_4 + H_2O_2) to render it hydrophilic, was suspended in the colloid-TiO_2 mixture for 48 hours so that the evaporation of the solvent resulted in an ordered face-centered cubic (fcc) assembly of the colloids with the interstices filled with the phase-controlled TiO_2 material. The self-assembled opal structures were then calcined at 500^{o}C at a ramp rate of 1^{o}C/min to remove the colloidal template and obtain the IO structure. Three samples, IOT 300, IOT 400 and IOT 500, with different pore sizes were prepared by using colloids of 300 nm (PS 300), 400 nm (PS 400) and 500 nm (PS 500), respectively.

2.2 Synthesis of IOT heterocomposites

In order to render the photocatalyst responsive to visible light, the IOT films were deposited with Bi-based semiconductor nanoparticles by Sequential Ionic Layer Adsorption Reaction (SILAR) method[11], wherein the films were sequentially dipped in the anionic and cationic precursors prepared at a 1:2 molar ratio, followed by calcination in order to obtain the crystalline phase of the IOTB films.

2.3 Synthesis of TiO_2 heterocomposite compact films

A TiO_2 compact film with a similar thickness to that of the IOT films was synthesized by optimizing a previously reported sol-gel dip coating method[12]. The film was then deposited with the Bi-based semiconductor nanoparticles using the same method as described above to obtain non-IO compact TiO_2-Bi-based (CTB) hetero-composite film.

2.4 Characterization methods

A JEOL JSM-7500F Scanning Electron Microscope (SEM) was used for electron microscopy observation and Energy Dispersive X-ray Spectroscopy (EDS) for quantitative analysis. An Olympus BX 61 microscope fitted with an Olympus XC50 camera was used to carry out optical microscopy observation. X-ray diffraction (XRD) patterns were taken using PANalytical X'PERT PRO Bragg-Brentano diffractometer using Cu Kα radiation (λ = 1.54184 Å) measured in 2θ angle range 20°-60°. Perkin Elmer 750S UV/Vis/NIR spectrophotometer was employed for absorptance measurements at 8° incidence, while an Avantes AvaSpec-2048-2 spectrophotometer coupled with an AvaLight-DH-S-BAL deuterium-halogen light source was used for reflectance measurements at normal incidence and detection wherein incident and reflected light were channeled through a bifurcated optical fiber.

2.5 Photocatalytic test

The IOTB (with different pore sizes) and CTB samples were tested for photocatalytic activity by the degradation of Rhodamine-B (RhB) in aqueous phase using a 300 W ELDIM-RFLX-ET101-01 EZ Reflex light source emitting a spectral range of 390-770 nm. Light was channeled through an Avantes FC-UV-200 optical fiber mounted on Avantes AFH-15 fiber holder onto the photocatalyst immersed in 4 ml of 2.0 µM RhB solution. After leaving the sample in the dark for 60 min to reach equilibrium, the test was allowed to continue for 6 hours, during which the photocatalytic degradation was analyzed every 60 min. by measuring the absorptance of the RhB solution using Analytik Jena-Specord 205 UV-VIS spectrophotometer.

3. RESULTS AND DISCUSSION

Highly ordered and homogeneous IO photonic structures are essential in order to exhibit a distinct SBG, at the edges of which the group velocity of light is reduced nearly to zero. In order to obtain ordered IO structures, a novel one-step co-assembly of template colloids and phase-controlled TiO_2 nanoparticles **(Fig. 1 (a))** was preferred to the conventional two-step process of assembling the colloids and then backfilling the interstices with the semiconductor material. The conventional process was often found to result in higher defect formation since the fragile opal template tends to get structurally disturbed during matrix material infiltration. Also, incomplete or excessive infiltration often tends to result in either a collapse of the photonic structure or a formation of overlayer.

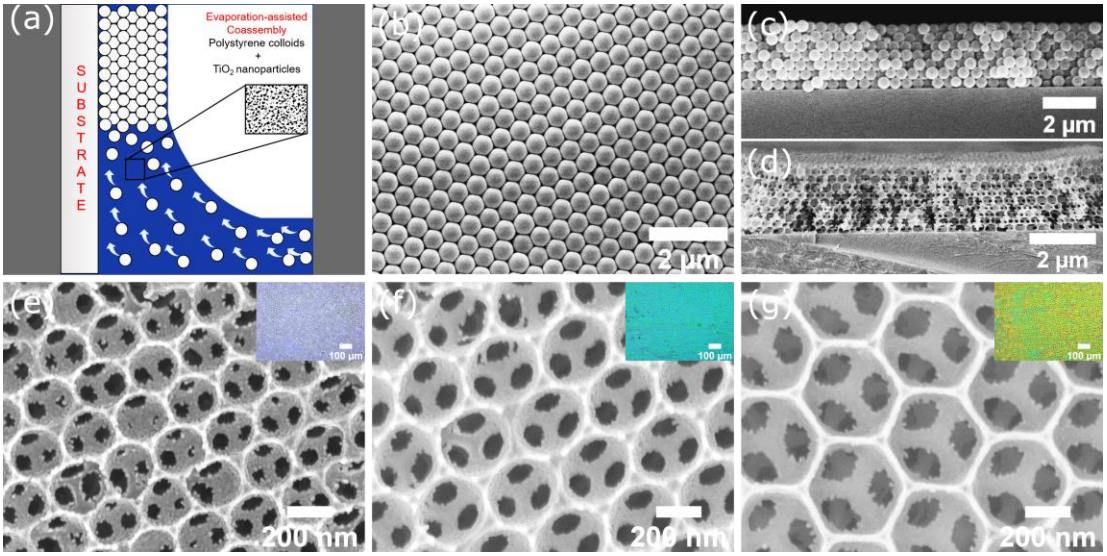

Figure 1. (a) Schematic illustration of the co-assembly of PS colloids and phase-controlled TiO_2 nanoparticles; (b) SEM image of PS 500 colloids-TiO_2 co-assembly; (c) Cross-section SEM image of the PS 500 colloid-TiO_2 co-assembly; (d) Cross section SEM image of IOT 500 obtained after calcination; (e-g) SEM images of IO photonic structures of IOT 300 (e), IOT 400 (f), IOT 500 (g), with their corresponding optical microscope images shown in the insets.

The co-assembly process adopted in this work avoided the delicate infiltration step, thus forming an ordered co-assembly **(Fig. 1 (b))**, that resulted in ordered IO structures after template removal **(Fig. 1 (e-g)).** Also, the use of phase-controlled crystalline-amorphous TiO_2 matrix material provided additional advantage striking the right equilibrium between providing stability to the structure (due to crystalline phase) and accommodating the stress arising from shrinkage during template removal by calcination (due to amorphous phase). Cross-section SEM images revealed that the film thickness was around 2 µm **(Fig. 1 (c,d))**.

SEM images of IOT 300, IOT 400 and IOT 500 **(Fig. 1 (e- g))** reveal homogeneous structures with pore sizes of 238 nm, 320 nm and 445 nm, respectively. This corresponds to a 15-20% shrinkage compared to the related colloid sizes. This is in accordance with previously reported results[13]. The corresponding optical microscope images shown in the insets with distinct colors corresponding to the SBG reflection confirm the high quality of the synthesized photonic structures. Since TiO_2 absorbs light only in the UV region, the IOT structures were deposited with Bi-based nanoparticles (25% by weight of TiO_2) in order to shift the absorptance of the photocatalysts to the visible region. SEM image shown in **Fig. 2 (a)** confirms the homogeneous deposition of the Bi-based semiconductor nanoparticles, while **Fig. 2 (b)** shows the shift in absorptance from UV region to the visible region after depositing the IOT structures with the visible light-responsive semiconductor. For comparison of photocatalytic activities, a non-structured compact TiO_2- Bi-based composite (CTB) film was synthesized **(Fig. 2 (c))**, with the similar quantity of Bi-based nanoparticles deposited as in the IO structures.

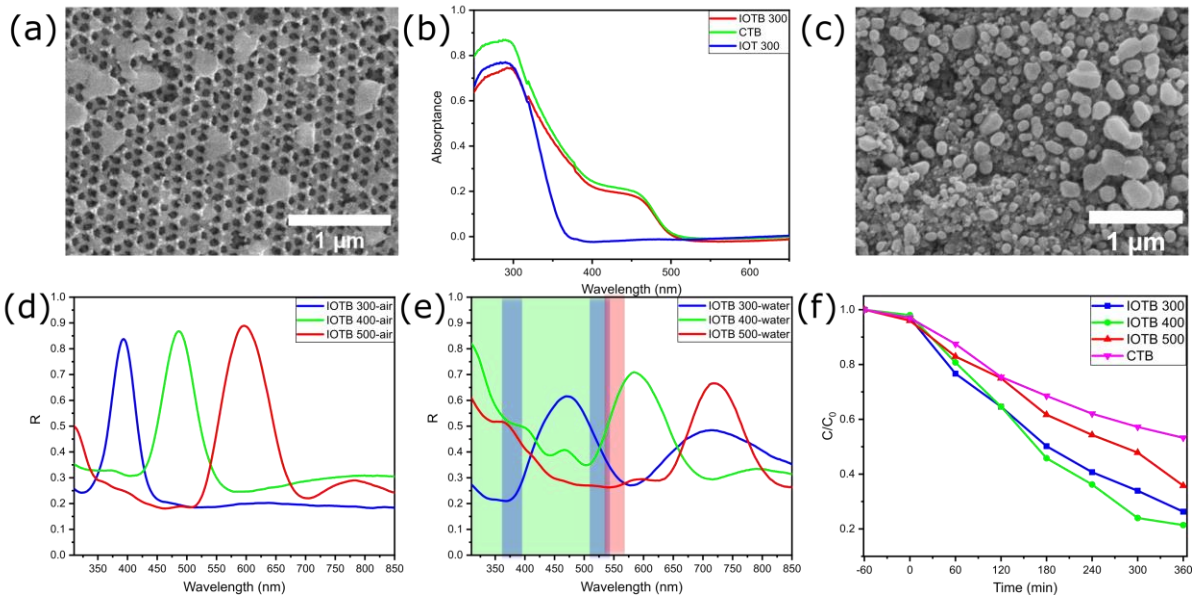

Figure 2. (a) SEM image of IOT 300 deposited with Bi-based nanoparticles (IOTB 300); (b) UV-Visible absorptance spectra of IOTB 300, CTB and IOT 300; (c) SEM image of a CTB sample; (d) Reflectance spectra in air of IOTB 300 (blue), IOTB 400 (green) and IOTB 500 (red); (e) Reflectance spectra in water of IOTB 300 (blue), IOTB 400 (green) and IOTB 500 (red); (f) Normalized concentration (C/C_0) as a function of time indicating the RhB degradation activity of IOTB 300 (blue), IOTB 400 (green), IOTB 500 (red) and CTB (magenta).

Reflectance spectral measurements in air **(Fig. 2 (d))** show that IOTB 300, IOTB 400 and IOTB 500 samples exhibit distinct SBG reflection peaks at 392, 487 and 597 nm, respectively. This corresponds to a gradual red shift of the SBG peak wavelength with an increase in the lattice parameter and pore size. The reflection peak positions can be theoretically estimated by Bragg's equation[14]:

$$\lambda = 2 \cdot \sqrt{2/3} \cdot D \cdot \sqrt{n_{matrix}^2(f) + n_{void}^2(1-f) - \sin^2\theta} \quad (1)$$

where λ is the wavelength of the reflection peak, D is the lattice parameter (here corresponding to the pore diameter), n_{matrix} is the average refractive index (RI) of TiO_2 host material and Bi-based nanoparticles, n_{void} is the RI of the medium

filling the pores (namely, air or water), f and (1-f) are the filling fractions of the matrix and pores, respectively, while ϑ is the angle between the incident light and the surface normal. It was observed that the experimentally determined positions of the SBG reflection peaks were lower than the theoretical predictions, which was probably due to a lower filling fraction of the host material, as reported in previous works[15], compared to the ideal filling fraction of $f = 0.26$ in a close-packed fcc arrangement. Since, photocatalytic degradation tests were done in aqueous phase, reflectance measurements were also performed after the pores were filled with water **(Fig. 2 (e))**. In water medium, the SBG reflection peaks red shifted due to the increase in refractive index of the filling medium from 1.0 (RI of air) to 1.33 (RI of water). It was also noted that the reflection peaks were lower in intensity and broader compared to those in air due to the lower RI contrast between the matrix and the pores filled with water.

The three IOTB samples were tested for photocatalytic RhB dye degradation and their activities were compared to that of non-structures CTB film. The comparison of photocatalytic efficiencies is represented in **(Fig. 2 (f))** in terms of normalized concentration (C/C_0) as a function of time of degradation, where C_0 is the initial concentration of RhB, while C is the concentration of RhB at time 't'. All the IO photocatalysts exhibited higher activity than that of the compact film. The comparison of degradation efficiencies of the photocatalysts ($(C_0\text{-}C)/C_0$*100%), after being normalized with respect to the amount of the visible light-responsive photocatalyst, revealed an average 70% increase in activity in IOTB samples compared to the non-structured CTB film. This can be justified by the assistance of slow photons in IO photonic structures in enhancing photocatalytic activity.

Among the three IOTB samples, IOTB 400 was found to exhibit the highest activity followed by IOTB 300 and then by IOTB 500. This difference in activity establishes the importance of accurately tuning the wavelengths of slow photons to the electronic absorption of the visible-light responsive Bi-based photocatalyst, in order to increase photocatalytic activity. In the case of IOTB 300, both the blue and red edge slow photon wavelengths (blue and red shades in Fig. 2 (e)) at ≈325 nm and ≈520 nm, respectively) were tuned in such a way that they overlap with the electronic absorption of the visible light photocatalyst (green shade in Fig 2 (e)). However, the absorption of visible light was reduced by the strong SBG reflection, which also fell within the absorption of the Bi-based photocatalyst, which explains its reduced photocatalytic activity compared to that of IOTB 400. In the case of IOTB 400, the blue edge slow photons (blue shade at ≈510 nm in Fig. 2 (e)) were tuned to the electronic absorption of the Bi-based photocatalyst, while, at the same time, the SBG reflection peak remained outside the absorption of the visible light photocatalyst. This explains the highest activity of IOTB 400 compared to the other two samples (20% and 10% higher than IOTB 500 and IOTB 300, respectively). Blue edge slow photons, although localized primarily in the lower RI medium (water), can still be utilized by the matrix material (photocatalyst) for enhancement of photocatalytic activity, as demonstrated through Rigorous Coupled Wave Analysis (RCWA) simulation studies[16]. The least activity of IOTB 500 can be explained by the fact that both blue and red edge slow photons are located far away from the electronic absorption of Bi-based photocatalyst, which reduces the impact of slow photons to a minimum. These results indicate that slow photons, when properly tuned to match with the electronic absorption of the photocatalyst, while simultaneously avoiding SBG reflection, can result in highly enhanced photocatalytic activity in IO photonic photocatalysts.

4. CONCLUSION

Slow photons in IO structures, originating from the reduction of group velocity of light at either edge of the photonic stop band gap, have immense potential in enhancing the photocatalytic activity of the nanostructured semiconductors. The challenges in benefitting fully from this potential lie firstly in synthesizing highly ordered photonic structures capable of generating a distinct SBG with slow photons at its edges and secondly in tuning the wavelengths of slow photons in such a way that they overlap with the electronic absorption of the photocatalyst. In this work, the first challenge was overcome by using a co-assembly method that resulted in ordered IO structures. The second challenge was overcome by varying the lattice parameter (and pore diameter), that resulted in the wavelengths of the slow photons being tuned to the electronic absorption of the Bi-based semiconductor nanoparticles, thereby enhancing light absorption and photocatalytic activity. In the present work, the activity of all IO structures, assisted by slow photons, was found to be around 70% higher than the non-structured composite. In addition, accurate tuning of the slow photons to the electronic absorption of the photocatalyst, while simultaneously avoiding SBG reflection resulted in a further 20% increase in photocatalytic activity. This work realized for a heterocomposite photocatalytic system in aqueous phase throws new light on the tuning strategies in aqueous phase, and opens new possibilities for utilizing the slow photon effect in other solar energy conversion processes like water splitting and CO_2 reduction.

ACKNOWLEDGEMENTS

T. L. M. acknowledges the perpetual support of the *Europe Occidentale Francophone* (EOF) and Andhra (India) Jesuit provinces for realizing this work. T. L. M. acknowledges a Student Conference Support grant from SPIE. S. R. M. was supported by the Maturation Fund of the Walloon Region and a BEWARE Fellowship of the Walloon Region (Convention n◦2110034). This research used resources of the Lasers, Optics & Spectroscopies (LOS) Technology Platform (https://platforms.unamur.be/los), the Physico-Chemical Characterization (PC^2) Technology Platform (https://platforms.unamur.be/pc2) and the Electron Microscopy Service (SME) of UNamur (http://www.unamur.be/en/sevmel). SME is a member of the Morphology - Imaging (MORPH-IM) Technology Platform of UNamur.

REFERENCES

[1] Kubacka, A., Fernandez-Garcia, M., Colon, G., "Advanced nanoarchitectures for solar photocatalytic applications", Chem. Rev. 112, 1555-1614 (2012).
[2] Xu, C., Anusuyadevi, P.R., Aymonier, C., Luque, R. and Marre, S., "Nanostructured materials for photocatalysis", Chem. Soc. Rev. 48, 3868-3902 (2019).
[3] Yablonovitch, E., "Inhibited spontaneous emission in solid-state physics and electronics", Phys. Rev. Lett. 58, 2059-2062 (1987).
[4] John, S., "Strong localization of photons in certain disordered dielectric superlattices", Phys. Rev. Lett. 58, 2486-2489 (1987).
[5] Joannopoulos, J.D., Johnson, S.G., Winn, J.N., Meade, R.D., [Photonic crystals, Molding the flow of light], Princeton Univ. Press, Princeton and Oxford, 94-121 (2008).
[6] Collins, G., Armstrong, E., McNulty, D., O'Hanlon, S., Geaney, H., O'Dwyer, C., "2D and 3D photonic crystal materials for photocatalysis and electrochemical energy storage and conversion", Sci. Technol. Adv. Mater. 17, 563-582 (2016).
[7] Chen, J.I.L., von Freymann, G., Choi, S.Y., Kitaev, V., Ozin, G.A., "Amplified photochemistry with slow photons", Adv. Mater. 18, 1915-1919 (2006).
[8] Pietron, J.J., DeSario, P.A., "Review of roles for photonic crystals in solar fuels photocatalysis", J. Photonics Energy 7, (2016).
[9] Liu, J., Zhao, H., Wu, M., Van der Schueren, B., Li, Y., Deparis, O., Ye, J., Ozin, G.A., Hasan, T., Su, B.L., "Slow photons for photocatalysis and photovoltaics", Adv. Mater. 29, 1605349 (2017).
[10] Phillips, K.R., Shirman, T., Shirman, E., Shneidman, A.V., Kay, T.M., Aizenberg, J., "Nanocrystalline precursors for the co-assembly of crack-free metal oxide inverse opals", Adv. Mater. 30, 1706329 (2018).
[11] Kumbhar, V.S., Lee, H., Lee, J., Lee, K., "Interfacial growth of the optimal $BiVO_4$ nanoparticles onto self-assembled WO_3 nanoplates for efficient photoelectrochemical water splitting", J. Colloid Interface Sci. 557, 478-487 (2019).
[12] Kim, D.J., Hahn, S.H., Oh, S.H., Kim, E.J., "Influence of calcination temperature on structural and optical properties of TiO_2 thin films prepared by sol–gel dip coating", Mater. Lett. 57, 355-360 (2002).
[13] Wu, M., Liu, J., Jin, J., Wang, C., Huang, S., Deng, Z., Li, Y., Su, B.-L., "Probing significant light absorption enhancement of titania inverse opal films for highly exalted photocatalytic degradation of dye pollutants", Appl. Catal. B 150-151, 411-420 (2014).
[14] Likodimos, V., "Photonic crystal-assisted visible light activated TiO_2 photocatalysis", Appl. Catal. B 230, 269-303 (2018).
[15] Wu, M., Jin, J., Liu, J., Deng, Z., Li, Y., Deparis, O., Su, B.-L., "High photocatalytic activity enhancement of titania inverse opal films by slow photon effect induced strong light absorption", J. Mater. Chem. A 1, 15491-15500 (2013).
[16] Deparis, O., Mouchet, S., Su, B.-L., "Light harvesting in photonic crystals revisited: why do slow photons at the blue edge enhance absorption? ", Phys. Chem. Chem. Phys. 17, 30525-30532 (2015).